TREE-GRASS SEGREGATION PATTERNS

Jian Yang[1] and Atsushi Yagi[2]

Received December 3, 2018

Abstract. In the preceding paper [21], we have introduced a tree-grass competition model for describing the kinematics of forest-grassland system and have found that the model admits some solutions showing coexistence of forest and grassland. The purpose of the present paper is then to investigate the boundary curves which partition forest patches and grassland patches. Through the investigations, we want to clarify the properties of segregation patterns of tree-grass coexistence in terms of forest connectivity. As it is very difficult to handle the very model equations in [21], we will make a reduction of the full model by extremely restricting the range where the parameters of equations can vary.

1 Introduction In the preceding paper [21], we have introduced a tree-grass competition model for describing the kinematics of forest-grassland system from a viewpoint of competitive system between trees and grass. We have also found after proving global existence of solutions that the model admits some solutions showing coexistence of forest and grassland which are partitioned each other by some clear boundary curves.

The purpose of the present paper is then to investigate the boundary curves partitioning forest and grassland, in other words, the properties of segregation patterns of trees and grass. It is, however, very difficult to handle the very model equations [21, (1.1)], for the dynamics of solutions change drastically depending on the parameters contained in the equations and the model equations actually contain so various parameters. Before investigating the segregation patterns, we want to make some restrictions on the parameters as follows.

First, we will consider an extreme case when the reaction rates μ and γ in the equation of grass of [21, (1.1)] are sufficiently large with respect to the diffusion rate d_g and when they are even sufficiently large with respect to the reaction rates f and h of the equation of old age trees. In such a case, as discussed in the next section, the model equations can reasonably be reduced into a smaller model. As a matter of fact, the reduced model coincides with the classical kinematic model of forest presented by Kuznetsov-Antonovsky-Biktashev-Aponina [11].

Second, we will choose only the mortality h of old age trees as a tuning parameter of our investigations fixing other parameters suitably. The reduced model given by (2.3) below with (2.4)-(2.5) coincides with the classical kinematic model of forest for which an extensive study has already been made, see [12, 17, 20], including the series of papers [1, 2, 3]. Among others, as reviewed in Section 3, the papers [1, 2, 3] clarified that the parameter h plays an important role for determining the dynamics of solutions.

By numerical computations, we shall find that three types of tree-grass segregation patterns, namely, high-connectivity forests, intermediate-connectivity forests and low connectivity forests, are created depending mainly on the mortality of old age trees. We shall also find some very interesting link between the characters of forest connectivity and the

2010 *Mathematics Subject Classification.* 35K55, 37L30, 74E15.
Key words and phrases. Segregation pattern, Numerical experiment, Forest connectivity.

instability-dimension of a unique homogeneous stationary solution, which is always unstable, showing coexistence of trees and grass (see Remark 3.1).

Those types of habitat patterns are actually observed in the real world by means of satellite imagery, which is a conventional remote-sensing method. For instance, we can find those patterns in a 100km height view of the Black Forest, Schwarzwald, Germany (see Google Earth). As in [7], monitoring data are statistically processed in order to investigate characters of habitat patterns. Devia-Murthya-Debnatha-Jhaa [4] reported that the forest connectivity is playing an important role of regulating its ecological factors such as species level biodiversity, wildlife movement, seed dispersion and so on.

2 Some Reduction of Tree-Grass Competition Model Let us argue a reduction of the original tree-grass competition model introduced in our preceding paper [21].

We begin with recalling the following tree-grass interaction system:

$$
\begin{cases}
\dfrac{\partial u}{\partial t} = \beta\delta w - (\lambda g + a v^2 + c)u - f u & \text{in } \Omega \times (0,\infty), \\
\dfrac{\partial v}{\partial t} = f u - h v & \text{in } \Omega \times (0,\infty), \\
\dfrac{\partial w}{\partial t} = d_w \Delta w - \beta w + \alpha v & \text{in } \Omega \times (0,\infty), \\
\dfrac{\partial g}{\partial t} = d_g \Delta g - \mu v g + \gamma \left(1 - \frac{g}{K}\right) g & \text{in } \Omega \times (0,\infty), \\
\dfrac{\partial w}{\partial n} = \dfrac{\partial g}{\partial n} = 0 & \text{on } \partial\Omega \times (0,\infty), \\
u(x,0) = u_0(x),\ v(x,0) = v_0(x),\ w(x,0) = w_0(x),\ g(x,0) = g_0(x) & \text{in } \Omega,
\end{cases}
\tag{2.1}
$$

in a two-dimensional bounded, $\mathcal{C}^2$ or convex domain Ω. Here, the unknown functions $u(x,t)$ and $v(x,t)$ denote tree densities of young and old age classes, respectively, at a position $x \in \Omega$ and at time $t \in [0,\infty)$. The unknown function $w(x,t)$ denotes a density of seeds in the air at $x \in \Omega$ and $t \in [0,\infty)$. Meanwhile, $g(x,t)$ denotes a density of grass at $x \in \Omega$ and $t \in [0,\infty)$. The third equation describes the kinetics of seeds; $d_w > 0$ is a diffusion constant, and $\alpha > 0$ and $\beta > 0$ are seed production and seed deposition rates, respectively. The first equation describes growth of young age trees; here, $0 < \delta \le 1$ is a seed establishment rate, $\lambda g + a v^2 + c$ is a mortality of young age trees which is proportional to the densities g and v^2 with coefficients $\lambda > 0$ and $a > 0$, $c > 0$ being a basic mortality. The second equation describes growth of old age trees; $f > 0$ is an aging rate from young age to old age, and $h > 0$ is a mortality. Finally, the fourth equation describes growth of grass that is basically given by a reaction-diffusion equation with a diffusion constant $d_g > 0$ and with a Fisher growth function $\gamma\left(1 - \frac{g}{K}\right) g$, where $\gamma > 0$ is a reaction rate and K is ground's capacity for grass, the term $-\mu v g$ denotes suppression by the trees with a coefficient $\mu > 0$. On w and g, the homogeneous Neumann conditions are imposed on the boundary $\partial\Omega$. Nonnegative initial functions $u_0(x) \ge 0$, $v_0(x) \ge 0$, $w_0(x) \ge 0$ and $g_0(x) \ge 0$ are given in Ω for all unknown functions. (Note that, for simplicity, the constant w_* in [21, (1.1)] was taken as $w_* = 0$ and the cubic growth function for g was replaced by a square growth function of Fisher type.)

We now want to consider the situation that the reaction rates μ and γ are sufficiently large with respect to the diffusion rate d_g. Then, the equation of density $g(x,t)$ of grass can be dominated by the reaction terms and reduced to the ordinary differential equation

$$
\frac{\partial g}{\partial t} = \left[-\mu v + \gamma\left(1 - \frac{g}{K}\right)\right] g \qquad \text{in } (0,\infty),
$$

for each spatial point $x \in \Omega$. Furthermore, we assume that the reaction rates μ and γ are sufficiently large with respect to the reaction rates f and h appearing in the equation of $v(x,t)$. Then, $g(x,t)$ reaches its stability much faster than $v(x,t)$. By the theory of ordinary differential equations, we observe (v being given) the following dynamics. If $\mu v > \gamma$, then $\frac{\partial g}{\partial t} < 0$ for every $0 < t < \infty$ and g tends to 0 as $t \to \infty$. If $\mu v \le \gamma$, then g tends to $\frac{K}{\gamma}(\gamma - \mu v)$ as $t \to \infty$. That is, g is represented as a function of v in the form

$$g = g(v) \equiv \begin{cases} \frac{K}{\gamma}(\gamma - \mu v) & \text{for} \quad 0 \le v < \frac{\gamma}{\mu}, \\ 0 & \text{for} \quad \frac{\gamma}{\mu} \le v < \infty. \end{cases} \tag{2.2}$$

Let us substitute $g(v)$ defined by (2.2) with the g in the equation for u of (2.1). Then, (2.1) is reduced to

$$\begin{cases} \dfrac{\partial u}{\partial t} = \beta\delta w - \varphi(v)u - fu & \text{in} \quad \Omega \times (0,\infty), \\ \dfrac{\partial v}{\partial t} = fu - hv & \text{in} \quad \Omega \times (0,\infty), \\ \dfrac{\partial w}{\partial t} = d_w \Delta w - \beta w + \alpha v & \text{in} \quad \Omega \times (0,\infty), \\ \dfrac{\partial w}{\partial n} = 0 & \text{on} \quad \partial\Omega \times (0,\infty), \\ u(x,0) = u_0(x),\ v(x,0) = v_0(x),\ w(x,0) = w_0(x), & \text{in} \quad \Omega, \end{cases} \tag{2.3}$$

where $\varphi(v) = av^2 + \lambda g(v) + c$.

Let us next investigate the behavior of $\varphi(v)$ for $0 \le v < \infty$. By the definition, $g(v)$ is a piecewise linear continuous function of v, therefore $\varphi(v)$ is a piecewise quadratic continuous function. For $\frac{\gamma}{\mu} \le v < \infty$, $\varphi(v) = av^2 + c$. When $a > \frac{K\lambda\mu^2}{2\gamma^2}$, $\varphi(v)$ takes a minimal value in the interval $0 \le v < \frac{\gamma}{\mu}$. Indeed, $\varphi(v)$ is written as

$$\varphi(v) = a\left(v - \frac{K\lambda\mu}{2a\gamma}\right)^2 + \frac{K\lambda(4a\gamma^2 - K\lambda\mu^2)}{4a\gamma^2} + c, \qquad 0 \le v < \frac{\gamma}{\mu}.$$

Meanwhile, when $a \le \frac{K\lambda\mu}{2\gamma^2}$, $\varphi(v)$ is monotonously decreasing in the interval $0 \le v < \frac{\gamma}{\mu}$. Therefore, in this case, $\varphi(v)$ takes a minimal value at $v = \frac{\gamma}{\mu}$ and its value is given as $\varphi\left(\frac{\gamma}{\mu}\right) = \frac{a\gamma^2}{\mu^2} + c$. In this way, $\varphi(v)$ has been seen to have a unique minimal value and to behave as a quadratic function for large variables v, although it is not smooth at the point $v = \frac{\gamma}{\mu}$.

It is then natural to expect that the dynamics of solutions to (2.3) must be quite analogous to that of solutions to the equations due to Kuznetsov-Antonovsky-Biktashev-Aponina [11] in which $\varphi(v)$ is just a quadratic function of the form

$$\varphi(v) = a'(v - b')^2 + c', \qquad 0 \le v < \infty, \tag{2.4}$$

a', b' and c' being some positive constants. In addition, we already know that when $\varphi(v)$ is as in (2.4) the solutions starting from initial functions $v_0(x)$ given in a neighborhood of b' remain in some other neighborhood of b' and perform very interesting asymptotic behavior. By these arguments, we may be allowed to approximate our non smooth quadratic-like

function $\varphi(v) = av^2 + \lambda g(v) + c$ as a square function of form (2.4) by setting

$$\begin{cases} a' = a, \quad b' = \dfrac{K\lambda\mu}{2a\gamma}, \quad c' = \dfrac{K\lambda(4a\gamma^2 - K\lambda\mu^2)}{4a\gamma^2} + c \qquad \text{when} \quad a > \dfrac{K\lambda\mu^2}{2\gamma^2}, \\ a' = a, \quad b' = \dfrac{\gamma}{\mu}, \quad c' = \dfrac{a\gamma^2}{\mu^2} + c \qquad \text{when} \quad a \le \dfrac{K\lambda\mu^2}{2\gamma^2}. \end{cases} \tag{2.5}$$

We have thus verified that, when the assumptions on μ, γ, d_g, f and h mentioned above are satisfied, the tree-grass model equations of (2.1) can reasonably be reduced to the model equations of (2.3). Here, the function $\varphi(v)$ is given by a square function of form (2.4) with the coefficients represented by (2.5).

3 Review of Known Analytical Results Let us review the known results for the problem (2.3) which are obtained by the series of papers [1, 2, 3].

I) Global Existence. In order to handle (2.3) analytically, we set an underlying Banach space X by

$$X \equiv \left\{ \begin{pmatrix} u \\ v \\ w \end{pmatrix} ; \ u, \, v \in L_\infty(\Omega) \ \text{ and } \ w \in L_2(\Omega) \right\}.$$

Then, (2.3) can be formulated as the Cauchy problem

$$\begin{cases} \dfrac{dU}{dt} + AU = F(U), \qquad 0 < t < \infty, \\ U(0) = U_0 \end{cases} \tag{3.1}$$

in X. Here, A denotes a closed linear operator of X of the form $A \equiv \mathrm{diag}\{f, h, \Lambda\}$, where Λ is a realization of the Laplace operator $-d_w\Delta + \beta$ in $L_2(\Omega)$ under the homogeneous Neumann boundary conditions, and A has the domain $\mathcal{D}(A) = L_\infty(\Omega) \times L_\infty(\Omega) \times H^2_N(\Omega)$, $H^2_N(\Omega)$ standing for the subspace of $H^2(\Omega)$ such that $u \in H^2_N(\Omega)$ if and only if $u \in H^2(\Omega)$ satisfies the homogeneous Neumann boundary conditions on $\partial\Omega$. Moreover, A is easily seen to be a sectorial operator of X with angle 0, namely, its spectrum is contained in the half real line $(0, \infty)$. Consequently, $-A$ generates an analytic semigroup e^{-tA} $(0 \le t < \infty)$ on X; actually, e^{-tA} is given as $e^{-tA} = \mathrm{diag}\{e^{-tf}, e^{-th}, e^{-t\Lambda}\}$.

In the meantime, $F(U)$ denotes a nonlinear operator of X of the form

$$F(U) \equiv \begin{pmatrix} \beta\delta w - \varphi(v)u \\ fu \\ \alpha v \end{pmatrix}, \qquad U = \begin{pmatrix} u \\ v \\ w \end{pmatrix} \in \mathcal{D}(F) = [L_\infty(\Omega)]^3.$$

Finally, U_0 denotes an initial value which is taken in X.

We can then apply the theory of semilinear abstract parabolic evolution equations (see [18, Chapter 4]). In fact, according to [1, Theorem 5.2], for any $0 \le u_0 \in L_\infty(\Omega)$, $0 \le v_0 \in L_\infty(\Omega)$ and $0 \le w_0 \in H^s(\Omega)$, where $s > 1$, (3.1) and hence (2.3) possesses a unique global solution such that

$$\begin{cases} 0 \le u, \, v \in \mathcal{C}([0, \infty); L_\infty(\Omega)) \cap \mathcal{C}^1((0, \infty); L_\infty(\Omega)), \\ 0 \le w \in \mathcal{C}([0, \infty); H^s(\Omega)) \cap \mathcal{C}^1((0, \infty); L_2(\Omega)) \cap \mathcal{C}((0, \infty); H^2_N(\Omega)). \end{cases} \tag{3.2}$$

II) Lyapunov Function.

Furthermore, as verified in [1, Section 7], the function

$$\Psi(U) = \int_\Omega \Big[\frac{\alpha}{2}(fu - hv)^2 + \frac{d_w f\beta\delta}{2}|\nabla w|^2 + h\alpha\Gamma(v) + \frac{f\beta^2\delta}{2}w^2 - (f\alpha\beta\delta)vw\Big]dx, \quad U \in \mathcal{D}(A),$$

becomes a Lyapunov function for all the solutions of (2.3), where $\Gamma(v) = \int_0^v [\varphi(v)v + fv]dv$ is a fourth order function for $0 \le v < \infty$ due to (2.4). In fact, let $U(t)$ be any solution of (2.3) lying in (3.2). Then, the value $\Psi(U(t))$ is monotonously decreasing for $0 \le t < \infty$. In addition, it holds that

$$\overline{U} \in \mathcal{D}(A) \text{ is a stationary solution (i.e., } A\overline{U} = F(\overline{U})\text{), if and only if } \Psi'(\overline{U}) = 0.$$

In particular, we notice that (2.3) admits no periodic solutions.

III) Asymptotic Behavior of Solutions. In general, when there exists a Lyapunov function for the global solutions, one can prove that the global solutions tend to a stationary solution as $t \to \infty$. In the present case, however, such a convergence is proved only for some special cases. We can analytically claim only that, for any global solution $U(t)$, there exists a temporal sequence $t_n \nearrow \infty$ for which it holds true that

$$\begin{cases} u(t_n) \to \overline{u} & \text{weak* in } L_\infty(\Omega), \\ v(t_n) \to \overline{v} & \text{weak* in } L_\infty(\Omega), \\ w(t_n) \to \overline{w} & \text{strongly in } L_2(\Omega). \end{cases}$$

See [2, Section 4] and [19].

In spite of these analytical results, our numerical computations show that any global solution tends weakly to a stationary solution as $t \to \infty$. Some of them are described in [2, Section 6].

IV) Structure of Stationary Solutions. Now, we are naturally interested in investigating the structure of stationary solutions, namely, $\overline{U}$ satisfying $A\overline{U} = F(\overline{U})$. We can use the theory of stationary solutions to semilinear abstract parabolic evolution equations (see [18, Section 6. 6]).

As a matter of fact, the structure of stationary solutions changes drastically depending on the parameters of the equations. We here want to focus in the case when

$$a'(b')^2 > 3(c' + f). \tag{3.3}$$

In addition, fixing all the parameters except h, we treat h as a control parameter and consider the four critical values $0 < h_* < h_- < h_+ < h^* < \infty$ of h which are defined by

$$h_* = \frac{f\alpha\delta}{a'(b')^2 + c' + f}, \qquad h^* = \frac{f\alpha\delta}{c' + f},$$

and

$$h_\pm = \frac{f\alpha\delta\left\{a'(b')^2 + 3(c' + f) \pm \sqrt{a'(b')^2[a'(b')^2 - 3(c' + f)]}\right\}}{2(c' + f)[a'(b')^2 + c' + f]},$$

respectively.

According [3, Section 2], we know under (3.3) the following results.

1) When $0 < h < h_*$, there exist two homogeneous stationary solutions $O = (0, 0, 0)$ and

$$P_+ = \left(\tfrac{h}{f}[b' + \sqrt{D}],\ b' + \sqrt{D},\ \tfrac{\alpha}{\delta}[b' + \sqrt{D}]\right), \quad \text{where } D = \tfrac{f\alpha\delta - (c'+f)h}{a'h}.$$

In this case, there exist no other (inhomogeneous) stationary solutions.

Furthermore, O is unstable and P_+ is stable. So, as $t \to \infty$, the solutions $U(t)$ of (2.3) generally converge to P_+.

2) When $h_* < h < h_-$, there exist three homogeneous stationary solutions O, P_+ and

$$P_- = \left(\tfrac{h}{f}[b' - \sqrt{D}],\ b' - \sqrt{D},\ \tfrac{\alpha}{\delta}[b' - \sqrt{D}]\right). \tag{3.4}$$

In addition, there exist many inhomogeneous stationary solutions.

In this case, O and P_+ are both stable. But P_- is unstable and its dimension of instability is finite.

3) When $h_- < h < h_+$, there exist the three homogeneous stationary solutions O and $P_\pm$ and there exist many inhomogeneous stationary solutions.

As before, O and P_+ are stable and P_- is unstable. But the dimension of instability of P_- is infinite.

4) When $h_+ < h < h^*$, the situation is similar to that of Case 2. Indeed, there exist the three homogeneous stationary solutions O and $P_\pm$ and there exist many inhomogeneous stationary solutions.

As in Case 2, O and P_+ are both stable, and P_- is unstable. The dimension of instability of P_- is finite.

5) When $h^* < h < \infty$, $O = (0, 0, 0)$ is a globally stable stationary solution. That is, as $t \to \infty$, every solution $U(t)$ of (2.3) tends to O; in particular, there exist no other stationary solutions.

Remark 3.1. When $h_* < h < h^*$, we have as seen the unstable homogeneous stationary solution P_- given by (3.4) whose tree density $\overline{v}$ is equal to $b' - \sqrt{D}$. Then, let us observe what a grass density is at $v = \overline{v}$ by mean of the simplified equation (2.2) of g. According to (2.5), if $a > \frac{K\lambda\mu^2}{2\gamma^2}$, then $b' < \frac{\gamma}{\mu}$, *a fortiori*, $\overline{v} < \frac{\gamma}{\mu}$. Hence, (2.2) yields that $g(\overline{v}) > 0$. Similarly, if $a \le \frac{K\lambda\mu^2}{2\gamma^2}$, then $\overline{v} < b' = \frac{\gamma}{\mu}$. Hence, (2.2) again yields that $g(\overline{v}) > 0$.

In this sense, P_- is considered to be a homogeneous stationary state showing coexistence of trees and grass. However, as announced in Cases 2, 3 and 4, such a homogeneous state can never be stable. □

4 Segregation Patterns This section is devoted to presenting our numerical results. Throughout the numerical computations, the plot is set as $\Omega = (0, 1) \times (0, 1)$ and discretized by 1024×1024. We adopted a central differencing scheme for the 2-dimensional space and the implicit method for the time-dependent computation. About the parameters, we refer, except a', to a series of the study on forest ecology [5, 6, 8, 9, 10, 13, 14, 15, 16, 22]. Indeed, those parameter values are listed in Table 1. Especially, we chose a value for a' that satisfies the condition shown by (3.3).

In this case, the four critical values of h are approximately computed as

$$h_* = 0.0012,\ h_- = 0.0026,\ h_+ = 0.0334,\ h^* = 0.0337,$$

respectively. For our numerical computations, we then choose three values $h_i\,(i = 1, 2, 3)$ of h in such a way that $h_* < h_1 < h_- < h_2 < h_+ < h_3 < h^*$. Indeed,

$$h_1 = 0.0019,\ h_2 = 0.018,\ h_3 = 0.0335.$$

Table 1: Model parameters (symbol, description, value and units)

Symbol	Description	Vaule	Units
d_w	Seeds diffusion rate	0.01	$m\,day^{-1}$
a'	-	20000	-
b'	Optimal seedling density	0.004	-
c'	Natural mortality of seedlings	0.0014	-
f	Growth rate of young trees	0.01	-
α	Producing rate of seeds	0.5	-
β	Implantation rate of seeds	1	-
δ	Surviving rate of seeds	0.0769	-

As for initial states, we want to design them by two manners. The first one is that we place a certain number of circular grass patches onto the homogeneous stable forest P_+. The second one is that we place a certain number of circular tree patches onto the homogeneous stable grassland O. The radii of tree patches and grass patches are both 0.025. Locations of centers of the circular patches are randomly selected. We choose the number of patches which can lead the system to tree-grass coexisting stable states for each value of h mentioned above.

1) When $h = h_1 = 0.0019$, the stable stationary homogeneous solution P_+ is (0.0013, $0.0071, 0.0035$). (A) and (C) of Figure 1 show the final stabilized states of v at $t = 1000$ starting from the initial states where 612 grass patches are placed onto P_+ and 232 tree patches are placed onto O, respectively. Green color stands for habitats of trees, while yellow color stands for vacant area (habitats of grass). Both of these two states have a tree-area ratio rating at 32%. Actually if we place less than 612 grass patches onto P_+ or more than 232 tree patches onto O, then the system finally tends to P_+.

Meanwhile, (B) and (D) of Figure 1 show the final stabilized states of v at $t = 1000$ starting from the initial states where 1400 grass patches are placed onto P_+ and 4 tree patches are placed onto O, respectively. Both of these two states have a tree-area ratio rating at 1%.

In all these states, each of the habitats of trees looks isolated, namely with relatively low spatial connectivity. We will consider these spatial patterns to be low-connectivity forests.

2) When $h = h_2 = 0.018$, the stable stationary homogeneous solution P_+ is (0.0085, $0.0047, 0.0024$). (A) and (C) of Figure 2 show the final stabilized states of v at $t = 1000$ starting from the initial states where 260 grass patches are placed onto P_+ and 580 tree patches are placed onto O, respectively. Both of these two states have a tree-area ratio rating at 59%. Actually if we place less than 260 grass patches onto P_+ or more than 580 tree patches onto O, then the system finally tends to P_+.

Meanwhile, (B) and (D) of Figure 2 show the final stabilized states of v at $t = 1000$ starting from the initial states where 580 grass patches are placed onto P_+ and 260 tree patches are placed onto O, respectively. Both of these two states have a tree-area ratio rating at 34%. Actually if we place more than 580 grass patches onto P_+ or less than 260 tree patches onto O, then the system finally tends to O.

In (A) and (C), habitats of trees are almost connected, but with not very high spatial connectivity. We will consider these spatial patterns to be intermediate-connectivity forests.

3) When $h = h_3 = 0.0335$, the stable stationary homogeneous solution P_+ is (0.0136, $0.0041, 0.0020$). (A) and (C) of Figure 3 show the final stabilized states of v at $t = 1000$

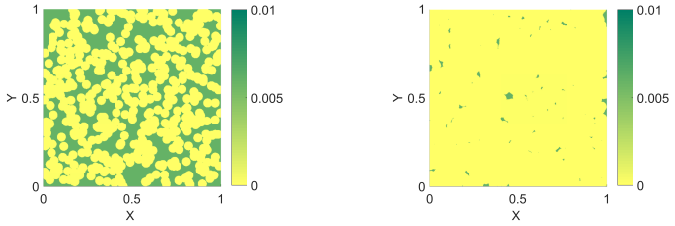

(A) (B)

(C) (D)

Fig. 1: Graphs of stabilized states of v at $t = 1000$ for $h = 0.0019$.

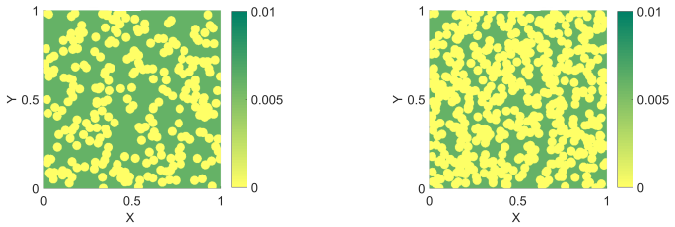

(A) (B)

(C) (D)

Fig. 2: Graphs of stabilized states of v at $t = 1000$ for $h = 0.018$.

starting from the initial states where 4 grass patches are placed onto P_+ and 1400 tree patches are placed onto O, respectively. Both of these two states have a tree-area ratio rating at 99%.

Meanwhile, (B) and (D) of Figure 3 show the final stabilized states starting from the initial states where 232 grass patches are placed onto P_+ and 612 tree patches are placed onto O, respectively. Both of these two states have a tree-area ratio rating at 68%. Actually if we place more than 232 grass patches onto P_+ or less than 612 tree patches onto O, then the system finally tends to O.

In all these states, habitats of trees look highly connected. We will consider these spatial patterns to be high-connectivity forests.

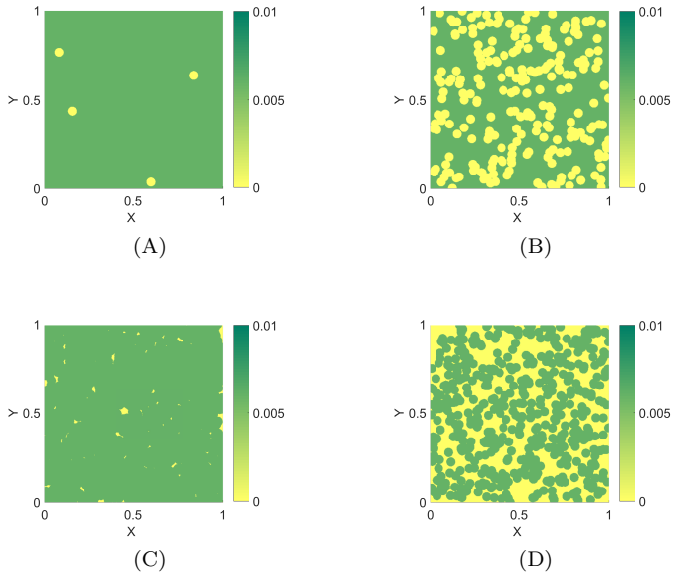

Fig. 3: Graphs of stabilized states of v at $t = 1000$ for $h = 0.0335$.

Our numerical results show a clear correlation between the mortality of old age trees h and the segregation patterns which are exhibiting tree-grass coexistence and are distinguished by different forest connectivity levels. We observe that, in order that tree-grass coexistence takes place, a forest with a relatively high mortality of old age trees needs a relatively high tree-area ratio, and its segregation pattern is of high connectivity. To the contrary, a forest with a relatively low mortality of old age trees needs only a relatively low tree-area ratio, and its segregation pattern is of low connectivity.

References

[1] L. H. Chuan and A. Yagi, *Dynamical system for forest kinematic model*, Adv. Math. Sci. Appli. **16** (2006), 393–409.

[2] L. H. Chuan, T. Tsujikawa and A. Yagi, *Asymptotic behavior of solutions for forest kinematic model*, Funkcial. Ekvac. **49** (2006), 427–449.

[3] L. H. Chuan, T. Tsujikawa and A. Yagi, *Stationary solutions to forest kinematic model*, Glasg. Math. J. **51**(2009), 1–17.

[4] B. S. S. Devia, M. S. R. Murthya, B. Debnatha, C. S. Jhaa *Forest patch connectivity diagnostics and prioritization using graph theory*, Ecological Modeling **251**(2013), 279–287.

[5] C. Favier, J. Chave, A. Fabing, D. Schwartz, M. A. Dubois, *Modeling forestsavanna mosaic dynamics in man-influenced environments: effects of fire, climate and soil heterogeneity*, Ecological Modelling **171**(2004), 85–102.

[6] M. Fenner, *The Ecology of Regeneration in Plant Communities*, CABI, 2000.

[7] S. Garca-Gigorro and S. Saura *Forest Fragmentation Estimated from Remotely Sensed Data: Is Comparison Across Scales Possible?*, Forest Science **51**(2005), 51–63.

[8] J. I. House, S. Archer, D. D. Breshears and R. J. Scholes, *Tree-grass interactions participants, conundrums in mixed woody-herbaceous plants systems*, J. Biogeography **30**(2003), 1763–1777.

[9] G. Kunstler, *Effects of competition on tree radial growth vary in importance but not in intensity along climatic gradients*, J. Ecology **99**(2011), 300–312.

[10] G. Kunstler, R. B. Allen, D. A. Coomes, C. D. Canham and E. F. Wright, *SORTIE/NZ model development*, Landcare Research New Zealand, 2011.

[11] Yu A. Kuznetsov, M. Ya. Antonovsky, V. N. Biktashev and A. Aponina, *A cross-diffusion model of forest boundary dynamics*, J. Math. Biol. **32** (1994), 219–232.

[12] G. Mola and A. Yagi, *A forest model with memory*, Funkcial. Ekvac. **52**(2009), 19–40.

[13] J. E. Ruiz *Effects of dispersal and insect herbivory on seedling recruitment of Dipteryx Oleifera Benth (Fabaceae) a tropical tree*, University of Michigan, 2008.

[14] M. Sankaran, J. Ratnam and N. P. Hanan, *Tree-grass coexistence in savannas revisited-insights from an examination of assumptions and mechanisms invoked in existing models*, Ecology Letters **7**(2004), 480–490.

[15] R. J. Scholes and S. R. Archer, *Tree-grass interactions in Savannas*, Annual Review Ecology Systematics **28**(1997), 517–544.

[16] J. Terborgh, K. Zhu and P. lvarez-Loayza, *How many seeds does it take to make a sapling?*, J. Ecol. Soc. Am **1**(2014), 1–33.

[17] A. Yagi, *Free boundary problem in forest model*, "Nonlinear Phenomena with Energy Dissipation", Gakkotosho, 2008, 425–440.

[18] A. Yagi, *Abstract Parabolic Evolution Equations and their Applications*, Springer, 2010.

[19] A. Yagi, *Open problems in forest model*, Proc. Workshop on Modern Mathematical Analysis and Applications, Hanoi University 2010, 1–9.

[20] A. Yagi and M. Primicerio, *A modified forest kinematic model*, Vietnam J. Math. Anal. **12**(2014), 107–118.

[21] J. Yang and A. Yagi, *Global existence for tree-grass competition model*, Sci. Math. Jpn., accepted for publication.

[22] L. Zhang, Z. Hu, J. Fan, D, Zhou and F. Tang, *A meta-analysis of the canopy light extinction coefficient in terrestrial ecosystems*, Frontiers of Earth Science **8**(2014), 599-609.

Communicated by *Koichi Osaki*

1 Department of Information and Physical Science, Osaka University, Suita, Osaka 565-0871, Japan
2 Professor Emeritus, Osaka University, Suita, Osaka 565-0871, Japan